

LUNASKA Experiment observational limits on UHE neutrinos from Centaurus A and the Galactic Centre

C. W. James^{1,2*}, R. J. Protheroe², R. D. Ekers³, J. Alvarez-Muñiz⁴,
R. A. McFadden^{3,5}, C. J. Phillips³, P. Roberts³, J. D. Bray^{2,3}

¹*IMAPP, Radboud University, Nijmegen, The Netherlands*

²*School of Chemistry & Physics, Univ. of Adelaide, Australia.*

³*Australia Telescope National Facility, CSIRO Astronomy & Space Science, Epping, Australia.*

⁴*Dept. Física de Partículas & IGFAE, Univ. Santiago de Compostela, Spain.*

⁵*School of Physics, Univ. of Melbourne, Australia.*

ABSTRACT

We present the first observational limits to the ultra-high energy (UHE) neutrino flux from the Galactic Center, and from Centaurus A which is the nearest active galactic nucleus (AGN). These results are based on our “Lunar UHE Neutrino Astrophysics using the Square Kilometer Array” (LUNASKA) project experiments at the Australia Telescope Compact Array (ATCA). We also derive limits for the previous experiments and compare these limits with expectations for acceleration and super-heavy dark matter models of the origin of UHE cosmic rays.

Key words: galaxies: individual: Centaurus A – galaxies: active – Galaxy: centre – neutrinos

1 INTRODUCTION

Arrival directions of the UHE cosmic rays (CR) detected by the Pierre Auger experiment above 5.6×10^{19} eV have been found to be statistically correlated with positions of nearby AGN (Abraham et al. 2007a), and a few of the arrival directions appear to be clustered around Centaurus A, our nearest active galactic nucleus at a distance of ~ 3.7 Mpc. This has led to speculation that Centaurus A may be responsible for some of the UHE CR. However, the flux is extremely low, and so the nature of the sources of UHE CR remains at present unknown.

As well as observing UHE CR directly, an alternative means of exploring the origin of UHE CR is to search for UHE neutrinos. Cosmic rays of sufficient energy will interact (e.g. via pion photo-production) with photons of the 2.725 K cosmic microwave background (CMB) radiation, with the resulting energy-loss producing a cut-off in the spectrum at around $\sim 10^{20}$ eV from a distant source (Greisen 1966; Zatsepin & Kuzmin 1966). These same interactions produce “cosmogenic” neutrinos from the decay of unstable secondaries (Stecker 1973; Stecker 1979; Berezhinsky & Zatsepin 1977; Protheroe & Johnson 1996; Engel et al. 2001). As well as these cosmogenic neutrinos, UHE neutrinos are also expected to be produced by acceleration and super-heavy dark matter (SHDM) sources of UHE CR, and some information on the CR spectrum at the sources is imprinted on

the spectrum of cosmogenic neutrinos (Protheroe 2004). Of course, neutrinos are not deflected by magnetic fields, and so should point back to where they were produced. See Protheroe & Clay (2004) and Falcke et al. (2004) for reviews of UHE CR production scenarios and radio techniques for high-energy cosmic ray and neutrino astrophysics.

1.1 The Lunar Cherenkov Technique

In our present work we use the lunar Cherenkov technique (Dagkesamanskii & Zheleznykh 1989), in which the Moon is used as a UHE neutrino target and Earth-based radio telescopes are used to detect coherent radio Cherenkov emission produced by neutrino-induced cascades in the lunar regolith. A high-energy particle interacting in a dense medium will produce a cascade of secondary particles which develops an excess negative charge by entrainment of electrons from the surrounding material and positron annihilation in flight. The charge excess is proportional to the number of particles in the electromagnetic cascade, which in turn is proportional to the energy of the primary particle. Askar’yan (1962) (see also Askar’yan 1965) first noted this effect and predicted the Cherenkov emission process in dense dielectric media to be coherent at radio frequencies where the wavelength is comparable to or larger than the dimensions of the shower, and this effect has been confirmed experimentally (Saltzberg et al. 2001). At wavelengths comparable to the width of the shower, the coherent emission is in a nar-

* E-mail: C.James@astro.ru.nl

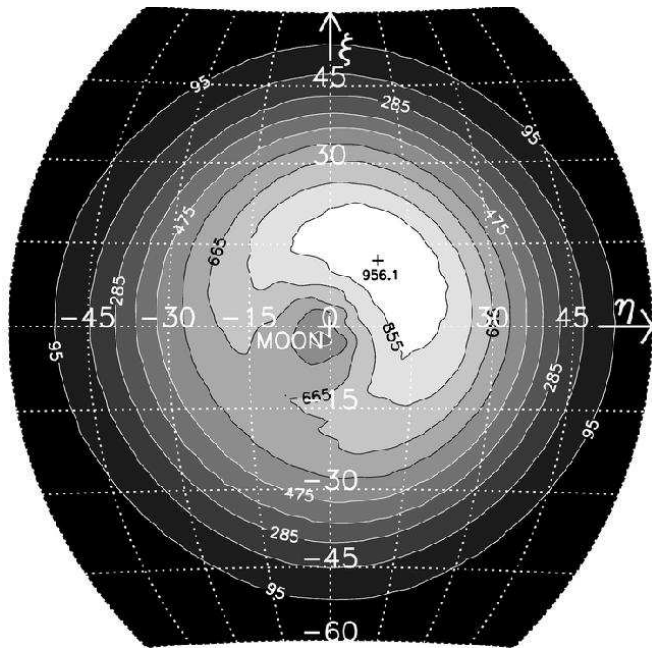


Figure 1. Contours of effective area (km^2) as a function of UHE neutrino arrival direction for 10^{23} eV neutrinos for limb-pointing configuration (May 2008). The ‘+’ marks the position of peak effective area; the Moon is at the center $(\eta, \xi) = (0, 0)$; telescope pointing direction $(\eta, \xi) = (0.183^\circ, 0.183^\circ)$.

row cone about the Cherenkov angle, while for wavelengths comparable to the shower length the coherent emission is nearly isotropic (Álvarez-Muñiz 2006).

The lunar Cherenkov technique aims to utilize the outer layers of the Moon, nominally the regolith which is a sandy layer of ejecta covering the Moon to a depth of ~ 10 m, as a suitable medium to observe the Askaryan effect. Since the regolith is comparatively transparent at radio frequencies, coherent Cherenkov emission from cascades due to sufficiently high-energy neutrino interactions in the regolith should be detectable as nanosecond-scale pulses by Earth-based radio-telescopes.

2 DESCRIPTION OF THE EXPERIMENT

The aim of the LUNASKA project is to develop further the lunar Cherenkov technique for UHE neutrino astronomy, and to influence the design of the Square Kilometer Array (<http://www.skatelescope.org/>) so that UHE neutrino observations may be possible. Our experiment was carried out at the ATCA which is an aperture synthesis telescope located at latitude -30° near Narrabri, Australia. It consists of six identical 22 m dishes of which we have used three with baselines ranging from ~ 100 m to ~ 750 m. The ATCA has a half-power beam-width that matches the lunar disk at 1.4 GHz, and it provided us with 600 MHz (1.2–1.8 GHz) of bandwidth. Being an array the ATCA also provided both strong timing discrimination against terrestrial radio-frequency interference (RFI), and gave a large effective area and high sensitivity while seeing the entire moon (Ekers et al. 2009). In order to perform a search for nanosecond-duration lunar Cherenkov pulses, we had to

build specialized hardware, including analogue de-dispersion filters as such pulses suffer dispersion in the Earth’s ionosphere – our experiment is the first to coherently correct for this before detection in real-time. To detect and store candidate events in real time we used field-programmable gate array (FPGA) based analog-to-digital converters developed by the Australia Telescope National Facility, each of which could digitize and perform simple logic on two data streams at a rate of 2.048 GHz. The signal was passed to both a running buffer of length 256 samples and a real-time trigger algorithm. We triggered independently, with a maximum rate of 1040 Hz, at each antenna. On fulfilling the trigger conditions, the buffer was returned to the control room and recorded. We calibrated the system sensitivity using the thermal emission from the lunar disk, and the system clocks at each antenna using correlated emission from the quasar 3C273. Full details of the experiment are given by James (2009) and James et al. (2010).

The observations described here cover two observing periods, February and May 2008. The February 2008 observations were tailored to target a broad ($\gtrsim 20^\circ$) region of the sky near the Galactic Center, both a potential accelerator of UHE CR and also a potential source of UHE CR, gamma-rays and neutrinos through its dark matter halo. Based on simulation results (James & Protheroe 2009a; James & Protheroe 2009b), we pointed the antennas at the lunar center in February to achieve the greatest total effective aperture and sensitivity to an isotropic or very broadly-distributed flux. Our May 2008 observing period targeted Centaurus A only, and by pointing the telescopes at the portion of the lunar limb closest to Centaurus A we achieved maximum sensitivity for this source. We recorded a total of 98307 3-fold coincidences within 4- μs windows, the majority of which, based on statistical arguments, could not come from random noise. Fitting these to far-field sources, ~ 60 appeared to come from the direction of the Moon. However, our 0.5 nanosecond timing resolution allowed us to show that these were all either near-field in origin, or were identifiable under visual inspection as long-duration, narrow-band RFI signals with little or no time-structure, occurring during short periods of intense RFI. Thus we excluded all candidates as being of lunar cosmic-ray or neutrino origin; cosmic rays interacting with lunar regolith with favourable geometry could also produce observable lunar Cherenkov emission.

We calculated the effective areas as described by James & Protheroe (2009b). This is shown in Fig. 1 for 10^{23} eV neutrinos and the limb-pointing configuration, and we see that the sensitivity has a characteristic ‘kidney’ shape peaking at $\sim 15^\circ$ away from the Moon along the line extending from the Moon’s center to the telescope pointing position on the lunar limb. For the center-pointing configuration (not shown), the sensitivity pattern forms an annulus, with peak exposure around 15° – 20° degrees from the Moon. For both configurations, the sensitivity pattern broadens with increasing primary particle energy as the increased strength of the pulses produced allows the telescopes to be sensitive to a wider range of interaction geometries. Combining the instantaneous aperture, e.g. as shown in Fig. 1, with the known telescope-pointing positions on the Moon and the Moon’s position itself at the time of observing, allows us to calculate the exposure $[A \times t](E_\nu; \alpha, \delta)$ (effective area-

time product) as a function of celestial coordinates (α, δ) . The exposure from our LUNASKA ATCA observations to UHE neutrinos is shown in Fig. 2 for 10^{23} eV. The nominal declination range of the ANITA observations is also given, and in this range the exposure of ANITA (not shown) dominates. The concentration of exposure about Centaurus A, and the broad Galactic Centre region (nominally Sagittarius A), both of which are outside ANITA’s sensitive declination range, is due to the targeting of these regions in our experiment by a careful choice of observing times.

3 RESULTS

The experiment with the greatest exposure to UHE neutrinos in the energy range above 10^{21} eV applicable here is the Antarctic Impulsive Transient Antenna Experiment (ANITA) (Barwick et al. 2006; Gorham et al. 2010) but this experiment is only sensitive to the declination range $-10^\circ \lesssim \delta \lesssim +15^\circ$ (indicated in Fig. 2). The IceCube experiment is primarily sensitive to the northern hemisphere, but has nevertheless been able to set limits up to 10^{18} eV for Centaurus A and the Galactic Center (Abbasi et al. 2009). The Pierre Auger observatory, although designed as a cosmic ray detector, is also sensitive to neutrinos, and a preliminary limit has been published for neutrinos from Centaurus A with energies up to 10^{20} eV (Tiffenberg et al. 2009). Other experiments for which we can obtain a neutrino flux limit from Centaurus A above 10^{17} eV are the pioneering experiment at Parkes (Hankins et al. 1996), the Goldstone Lunar UHE Neutrino Experiment (GLUE) (Gorham et al. 2004), the NuMoon observations using the Westerbork interferometer (Scholten et al. 2009), and the Radio Ice Cherenkov Experiment (RICE) (Kravchenko et al. 2006). The directional dependence of the exposures of the original Parkes experiment and GLUE were calculated previously by James & Protheroe (2009b).

The NuMoon lunar Cherenkov observations at Westerbork are reported by Scholten et al. (2009). While neither Centaurus A nor the Galactic Centre was explicitly targeted, lunar Cherenkov experiments operating at an order of magnitude lower frequency than ATCA, such as the Westerbork array, are expected to be more sensitive at energies above 10^{23} eV (Scholten et al. 2009). We simulated the sensitivity to isotropic 10^{23} eV neutrinos for the NuMoon experimental configuration of two fan beams on different sides of the Moon, each with 4 frequency sub-bands of width 65 MHz centred on 123, 137, 151 and 165 MHz covering 1/3 of the Moon. Adopting a 10 m thick regolith with a denser sub-regolith layer, and using the triggering criteria as described by Scholten et al. (2009) we found a sensitivity a factor of ~ 10 lower than that calculated by Scholten et al. (2009). We are able to closely reproduce the published NuMoon result by instead simulating one continuous bandwidth with a 240 kJy threshold (artificially improving the sensitivity by a factor of 5) and letting the depth of the top regolith layer become infinite (gaining a further factor of 2).

Using the method of James & Protheroe (2009b), but taking account of the fan beams of the Westerbork antennas, the frequency sub-bands and triggering criteria, our simulations show that for NuMoon the instantaneous neutrino directional aperture rises rapidly from zero at 0° from the

Moon to a peak at $\sim 40^\circ$ away from the Moon, and then drops to zero at $\sim 100^\circ$ away from the Moon. To calculate the limit for Centaurus A we obtained the observation dates from Buitink (2009), and on two of these dates the Moon happened to be $\sim 45^\circ$ from Centaurus A. Because only the observation dates (not the times) were available we assumed uniform lunar coverage by the two beams, but reduced by 1/3 since each beam covered $\sim 1/3$ of the Moon. We calculated the neutrino sky coverage of NuMoon by integrating the instantaneous neutrino directional aperture for the positions of the Moon on the observation dates and obtained the NuMoon sensitivity for 10^{23} eV neutrinos from Centaurus A. We obtained the sensitivity for the Galactic Centre using the same method.

RICE was a Cherenkov radio experiment embedded in Antarctic ice at the South Pole and had a much lower neutrino energy threshold than the three lunar Cherenkov experiments, albeit with only a slowly-increasing exposure with neutrino energy. However, it had a very long observation time of several years as compared to several days for the lunar Cherenkov experiments and this compensates for its lower instantaneous effective aperture. RICE was mostly sensitive to down-going neutrino events, and so to declinations $\delta < 0^\circ$. The directional sensitivity pattern at 10^{22} eV (Besson 2008) shows that its sensitivity to Centaurus A and the Galactic Centre are respectively 1.0 and 1.4 times its average sensitivity to a source in the southern hemisphere. Taking this directional sensitivity as representative for all energies, and the energy dependence of the exposure to a diffuse flux as given by Kravchenko et al. (2006) we can thus calculate the exposure of RICE to these point sources. Since the isotropic exposure is only given to 10^{22} eV in Kravchenko et al. (2006), in calculating the directional exposure we use a log-linear scaling and assume an isotropic exposure of 6.3×10^{17} cm² s sr to 10^{23} eV neutrinos.

The individual and total exposures of the GLUE, RICE, NuMoon and LUNASKA experiments to UHE ν from Centaurus A and Sgr A are given in Table 1 for 10^{21} , 10^{22} , and 10^{23} eV. Model-independent 90% confidence limits to the neutrino flux at energy E_ν from putative point sources at positions (α, δ) can be obtained from the exposure using $E_\nu F_\nu(E_\nu) \leq 2.3/[A \times t](E_\nu; \alpha, \delta)$. The errors in the LUNASKA exposures given in Table 1 reflect the in-quadrature addition of two dominant factors - uncertainties in the absolute detector thresholds, and the unknown properties of the lunar regolith. An estimate of the former is described in our earlier publication (James et al. 2010). To estimate uncertainties due to regolith properties, we use the measured variation in moon rock radio absorption and density (Olhoeft & Strangway 1975). The mare have a dense highly radio-absorbent regolith, and we vary the fraction of the part of the lunar surface relevant for lunar Cherenkov events due to neutrinos from Centaurus A and the Galactic Centre. For our “best-case regolith” estimate we use a 0% mare fraction, since there are very few mare regions in the lunar South where events from Centaurus A would be located. For our “worst-case regolith” estimate, we use a 30% mare fraction, which is approximately twice the lunar average and would correspond to the near side of the Moon being uniformly covered with mare. The mare regions in our “worst case regolith” are modelled as having density $\rho = 3.0$ g/cm³ and field attenuation length $\ell = 2.94$ m at 1 GHz, while “best

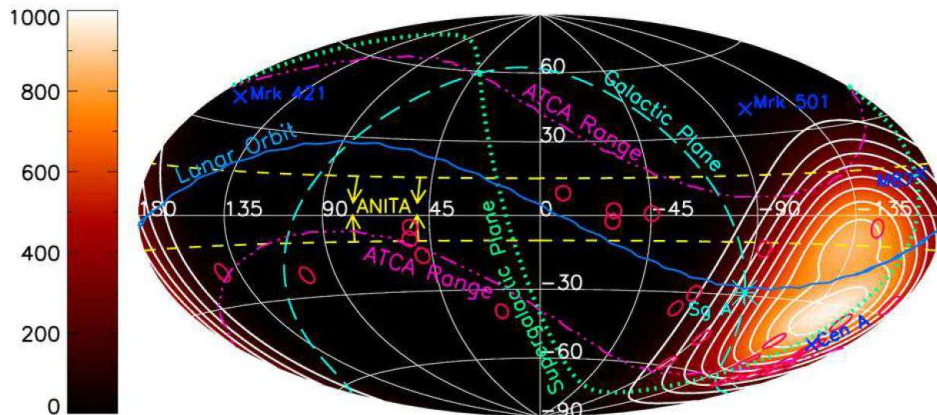


Figure 2. The exposure (km²-days) of the 2008 LUNASKA UHE ν detection experiment using the ATCA to 10^{23} eV neutrinos. The small circles show the directions of UHE CR events above 5.6×10^{19} eV detected by Auger (Abraham et al. 2007a). The positions of the Galactic Centre and four important AGN are indicated by crosses labelled “Sgr A*”, “Mrk 421”, “Mrk 501”, “M87” and “Cen A”. The Galactic plane and Supergalactic plane are indicated by long-dashed and dotted curves, respectively. The region of sky accessible to lunar Cherenkov observations using the ATCA is between the two chain curves labelled “ATCA RANGE”. In the declination range $-10^\circ \lesssim \delta \lesssim +15^\circ$ (between the short dashed curves labelled “ANITA”) the exposure of ANITA far exceeds that of other experiments, but for clarity has not been plotted.

case regolith” is modelled with $\rho = 1.8$ and $\ell = 22$ m. Finally, we assume a $(10 \pm 10)\%$ increase in aperture due to the interactions of secondary μ and τ , as calculated for other similar experiments by James & Protheroe (2009a). Our error estimates do not account for the extreme uncertainty in the UHE neutrino interaction cross-sections – these are so poorly understood at these energies that determining them is an experimental goal as much as a calculation uncertainty. Given the strong proportionality between cross-section and effective area/sensitivity for this and similar experiments (James & Protheroe 2009a), our flux limit is really a limit on the flux—cross section product.

4 SUMMARY AND CONCLUSION

In Fig. 3 we show the all-flavor neutrino flux limits for Centaurus A. With Centaurus A only 3.7 Mpc away, and with the pion photo-production energy-loss distance on the CMB minimizing at ~ 12 Mpc above 10^{11} GeV (e.g. Protheroe 2004) for rectilinear propagation one would observe UHE CR almost unattenuated by pion photo-production interactions on the CMB. Rieger & Aharonian (2009) suggest that shear acceleration along the kpc jet may accelerate protons beyond 5×10^{19} eV. The magnetic field of Centaurus A’s giant lobes (Feain et al. 2009) may also provide an environment suitable for acceleration of UHE CR (Benford & Protheroe 2008; Hardcastle et al. 2009).

Cuoco & Hannestad (2008) have predicted the flux of UHE neutrinos from the Centaurus A core (‘CH08’ in Fig. 3) using a model of an optically thick pion photo-production source described by Mannheim et al. (2001). They assume that accelerated cosmic ray protons are perfectly magnetically contained, and escape only through photo-hadronic interactions which convert them to neutrons. Under their model, the observed $E^{-2.7}$ spectrum of cosmic rays requires a $E^{-1.7}$ proton injection spectrum within the source, which would also produce a $E^{-1.7}$ spectrum of neutrinos; however,

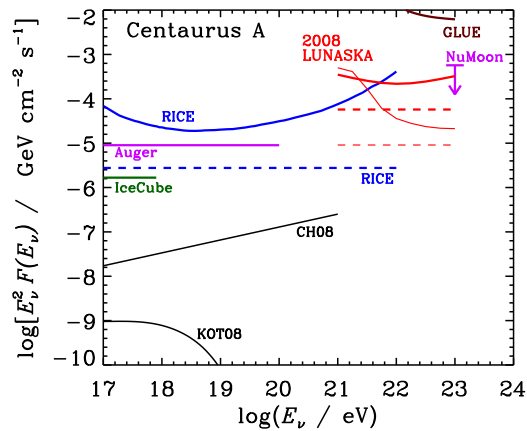


Figure 3. Neutrino flux limits for Centaurus A from our 2008 LUNASKA ATCA experiments, and based on the GLUE, NuMoon and RICE, as well as published results from IceCube and Auger experiments. Limits are shown as integrated limits to a E_ν^{-2} spectrum (dashed lines), as well as model-independent limits (solid curves) where available – the NuMoon limit is model-independent. For the LUNASKA ATCA limit we show results from standard modeling (thick curve and thick dashed line) and using a toy model of small-scale lunar surface roughness (thin curve and thin dashed line) as described in Appendix B of James et al. (2010) – the abrupt transition near 2×10^{21} eV is a model artifact. Neutrino flux predictions of two AGN models for UHE CR production as labeled: KOT09 (Kachelriess et al. 2009a); CH08 (Cuoco & Hannestad 2008).

these assumptions may break down towards the upper end of the energy range considered here. They normalize the CR flux by assuming that 2 of the Auger events above 5.6×10^{19} eV are from Centaurus A, and determine the relative normalization between the CR and neutrino fluxes through Monte Carlo simulations of $p-\gamma$ interactions in the accelera-

Table 1. Experimental exposures (km²-days) of GLUE, RICE, NuMoon (Westerbork) and the LUNASKA ATCA observations to UHE neutrinos at discrete energies from the Galactic Center and Centaurus A.

E_ν (eV)	Galactic Centre				Centaurus A			
	GLUE	RICE	NuMoon	ATCA	GLUE	RICE	NuMoon	ATCA
10^{21}	0.5	47	0	$3.2^{+2.7}_{-1}$	0.015	35	0	$7.6^{+6.4}_{-2.5}$
10^{22}	14	86	0	59^{+32}_{-15}	2.1	65	0	122^{+66}_{-31}
10^{23}	175	157	73.2	450^{+102}_{-104}	43	121	467	819^{+186}_{-189}

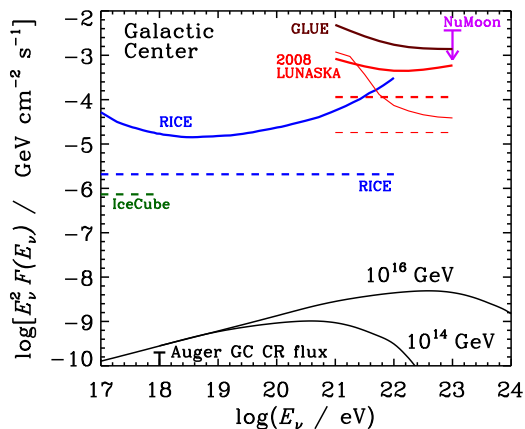


Figure 4. Neutrino flux limits for the Galactic Centre from our 2008 LUNASKA ATCA experiments, and based on the GLUE, NuMoon and RICE experiments, and published IceCube limit. Neutrino limits are shown as integrated limits to a E_ν^{-2} spectrum (dashed lines), as well as model-independent limits (solid curves) where available – the NuMoon limit is model-independent. Thin curves for the LUNASKA ATCA result are for modelling using a toy model of small-scale lunar roughness. SHDM models (see text) with $M_X = 10^{14}$ GeV and $M_X = 10^{16}$ GeV (as labeled). Limit at 10^9 GeV: Auger limit on the *cosmic ray* flux from a point source at the Galactic Centre (Abraham et al. 2007b).

tion region using the SOPHIA event generator (Mücke et al. 2000).

Kachelriess et al. (2009a) also assume a CR flux composed of protons, normalized with the assumption that 2 of the UHE Auger events are from Centaurus A. They consider several possible proton injection spectra, with acceleration occurring either in regular electromagnetic fields close to the core of the AGN or through shock acceleration in the jets, and predict the resulting neutrino and gamma-ray spectra for each. The jet acceleration scenarios are excluded by TeV gamma-ray data (Kachelriess et al. 2009b), and we plot (‘KOT09’ in Fig. 3) their result for acceleration near the core with an E^{-2} proton injection spectrum.

In Fig. 4 we show all-flavor neutrino flux limits for the Galactic Center. We consider the possibility that the Galaxy’s dark matter halo is composed partly of super-heavy dark matter, which decays or annihilates into particles which cascade into neutrinos, photons, and nucleons. We use fragmentation functions of Aloisio et al. (2004) for $M_X = 10^{16}$

GeV and normalize the sum of the gamma-ray plus nucleon components to the Auger limit on the *cosmic ray* flux from a point source at the Galactic Centre (Abraham et al. 2007b). We plot the corresponding neutrino flux shown as the curve labeled “ 10^{16} GeV”. We also show the expected neutrino flux assuming $M_X = 10^{14}$ GeV. Of course whether or not the neutrino (and cosmic ray) flux from SHDM annihilation appears point-like will depend on the radial distribution of the dark matter halo (Evans et al. 2002). If this distribution is cusped the angular distribution will be narrow, approximating to a point source, but in the case of other models the angular distribution can be broadened to up to $\sim 60^\circ$ half width.

In comparison with experiments such as ANITA, our methods to improve sensitivity to certain specifically targeted regions were successful. We have reported the first neutrino flux limits above 10^{21} eV from Centaurus A and the Galactic Center. For Centaurus A, the limit from our 2008 LUNASKA experiments using the ATCA is currently the strongest at primary neutrino energies of 5×10^{21} eV and above. While not ruling out any of the current theories of UHE CR production we have proved the viability of the lunar Cherenkov technique for targeted observation of specific UHE neutrino source candidates.

ACKNOWLEDGMENTS

The Australia Telescope Compact Array is part of the Australia Telescope which is funded by the Commonwealth of Australia for operation as a National Facility managed by CSIRO. This research was supported by the Australian Research Council’s Discovery Project funding scheme (project numbers DP0559991 and DP0881006). J.A-M. thanks Xunta de Galicia (INCITE09 206 336 PR) and Consellería de Educación (Grupos de Referencia Competitivos – Consolider Xunta de Galicia 2006/51), and Ministerio de Ciencia e Innovación (FPA 2007-65114 and Consolider CPAN) for financial support, and CESGA (Centro de SuperComputación de Galicia) for computing resources and assistance.

REFERENCES

- Abbasi R. et al., 2009, Phys. Rev. Lett., 103, 221102
- Abraham J. et al. (Auger Collaboration), 2007, Science 318, 938
- Abraham J. et al. (Auger Collaboration), 2007, Astropart. Phys. 27, 244

- Aloisio R., Berezinsky V. & Kachelriess M., 2004, *Phys. Rev. D*, 69, 094023
- Álvarez-Muñiz J., Marques E., Vazquez R. A., Zas E., 2006, *Phys. Rev. D* 74, 023007
- Askar'yan G. A., 1962, *Sov. Phys. JETP*, 14, 441
- Askar'yan G. A., 1965, *Sov. Phys. JETP*, 48, 988
- Barwick S. W. et al., 2006, *Phys. Rev. Lett.*, 96, 171101
- Benford G., Protheroe R. J., 2008, *MNRAS*, 383, 663
- Berezinsky V. S. & Zatsepin G. T., 1977, *Sov. J. Uspekhi*, 20, 361
- Besson D., 2008, private communication
- Buitink S., Radio emission from cosmic particle cascades (Doctoral Thesis), Radboud University Nijmegen, 2009
- Cuoco A. & Hannestad S., 2008, *Phys. Rev. D*, 78, 023007
- Dagkesamanskii R. D., Zheleznykh I. M., 1989, *Sov. Phys. JETP Lett.* 50, 233
- Ekers R.D., James C.W., Protheroe R.J., McFadden R.A., 2009, *Nucl. Instr. and Meth. in Phys. Res. A*, 604, S106
- Engel R., Seckel D., Stanev T., 2001, *Phys. Rev. D* 64, 093010
- Evans N. W., Ferrer F., Sarkar S., 2002, *Astroparticle Physics*, 17, 319
- Falcke H., Gorham P., Protheroe R.J., 2004, *New Astron. Rev.* 48, 1487
- Feain I. J., et al., 2009, *ApJ*, 707, 114
- Gorham P. W. et al., 2004, *Phys. Rev. Lett.*, 93, 041101
- Gorham P. W. et al., 2010, preprint arXiv:1003.2961
- Greisen K., 1966, *Phys. Rev. Lett.* 16, 748
- Hankins T.H., Ekers R.D., O'Sullivan J.D., 1996, *Mon. Not. Royal Astron. Soc.*, 283, 1027
- Hardcastle M. J., Cheung C. C., Feain I. J., Stawarz L., 2009, *MNRAS*, 393, 1041
- James C.W., Ultra-high energy particle detection with the lunar Cherenkov technique (Doctoral Thesis), University of Adelaide, 2009; available from <http://digital.library.adelaide.edu.au/dspace/handle/2440/57706>
- C. W. James, Ekers R.D., Álvarez-Muñiz J., Bray J.D., McFadden R.A., Phillips C.J, Protheroe R.J., Roberts P., 2010, *Phys. Rev. D*, vol. 81, Issue 4, id. 042003
- James C. W., Protheroe R. J., 2009, *Astropart. Phys.*, 30, 318
- James C. W., Protheroe R. J., 2009, *Astropart. Phys.*, 31, 392
- Kachelriess M., Ostapchenko S., Tomas R., 2009, *New J. of Phys.*, 11, 065017
- Kachelriess M., Ostapchenko S., Tomas R., 2009, *Int.J.Mod.Phys.D*18:1591-1595
- Kravchenko I. et al., 2006, *Phys. Rev. D* 73, 082002
- Mannheim K., Protheroe R.J., Rachen J.P., 2001, *Phys. Rev. D* 63, 023003
- Mücke A., Engel R., Rachen J. P., Protheroe R. J., Stanev T., 2000, *CoPhC*, 124, 290
- Olhoeft G.R., Strangway D.W., 1975, *Earth and Plan.Sci.Lett.*, 24, 394
- Protheroe R.J., 2004, *Astropart. Phys.* 21, 415
- Protheroe R.J., Clay R.W., 2004, *PASA* 21, 1
- Protheroe R.J., Johnson P.A., 1996, *Astropart. Phys.* 4, 253
- Rieger F. M., Aharonian F. A., 2009, *A&A*, 506, L41
- Stecker F. W., 1973, *Ap&SS*, 20, 47
- Stecker F. W., 1979, *ApJ*, 228, 919
- Saltzberg D., Gorham P., Walz D., Field, C., Iverson R., Odian A., Resch G., Schoessow P., Williams D., 2001, *Phys. Rev. Lett.* 86, 2802
- Scholten O., Buitink S., Bacelar J., Braun R., de Bruyn A.G., Falcke H., Singh K., Stappers B., Strom R.G., al Yahyaoui R., 2009, *Phys. Rev. Lett.* 103, 191301
- Tiffenberg J. et al. (Auger Collaboration), 2009, *Proc. of the 31st Intl. Cosmic Ray Conf.*, Lodz
- Zatsepin G.T., Kuzmin V.A., 1966, *JETP Lett.* 4, 78